William J. Richardson
Department of Biomedical Engineering,
Texas A&M University,
337 Zachry Engineering Center,
3120 TAMU,
College Station, TX 77843

Richard P. Metz
Department of Systems Biology and
Translational Medicine,
Texas A&M Health Science Center,
336 Reynolds Medical Building,
College Station, TX 77843

Michael R. Moreno
Department of Biomedical Engineering,
Texas A&M University,
337 Zachry Engineering Center,
3120 TAMU,
College Station, TX 77843

Emily Wilson
Department of Systems Biology
and Translational Medicine,
Texas A&M Health Science Center,
336 Reynolds Medical Building,
College Station, TX 77843

James E. Moore, Jr.
Department of Biomedical Engineering,
Texas A&M University,
337 Zachry Engineering Center,
3120 TAMU,
College Station, TX 77843

A Device to Study the Effects of Stretch Gradients on Cell Behavior

Mechanical forces are key regulators of cell function with varying loads capable of modulating behaviors such as alignment, migration, phenotype modulation, and others. Historically, cell-stretching experiments have employed mechanically simple environments (e.g., uniform uniaxial or equibiaxial stretches). However, stretch distributions in vivo can be highly non-uniform, particularly in cases of disease or subsequent to interventional treatments. Herein, we present a cell-stretching device capable of subjecting cells to controllable gradients in biaxial stretch via radial deformation of circular elastomeric membranes. By including either a defect or a rigid fixation at the center of the membrane, various gradients are generated. Capabilities of the device were quantified by tracking marked positions of the membrane while applying various loads, and experimental feasibility was assessed by conducting preliminary experiments with 3T3 fibroblasts and 10T1/2 cells subjected to 24 h of cyclic stretch. Quantitative real-time PCR was used to measure changes in mRNA expression of a profile of genes representing the major smooth muscle phenotypes. Genes associated with the contractile state were both upregulated (e.g., calponin) and downregulated (e.g., α-2-actin), and genes associated with the synthetic state were likewise both upregulated (e.g., SKI-like oncogene) and downregulated (e.g., collagen III). In addition, cells aligned with an orientation perpendicular to the maximal stretch direction. We have developed an in vitro cell culture device that can produce non-uniform stretch environments similar to in vivo mechanics. Cells stretched with this device showed alignment and altered mRNA expression indicative of phenotype modulation. Understanding these processes as they relate to in vivo pathologies could enable a more accurately targeted treatment to heal or inhibit disease, either through implantable device design or pharmaceutical approaches. [DOI: 10.1115/1.4005251]

Keywords: mechanobiology, stretching device, non-uniform stretch

Introduction

Mechanical loads are key regulators of arterial cell function in both normal and disease conditions. Thus, in order to develop adequate treatments for pathology, there is a need to link specific mechanical stimuli to particular cell responses related to disease. This task is made difficult partly by the complex mechanical environment within the arterial wall, resulting from large deformation of pre-stressed, heterogeneous, and anisotropic material. In an effort to identify the effects this loading has on arterial cells of all types, researchers over the past few decades have effectively employed a variety of experiments that sought to isolate mechanical stimuli. In general, those experiments subjected cells to a simplified mechanical load such as shear stress over an endothelial cell (EC) monolayer in a parallel plate flow chamber (e.g., see Ref. [1]), or uniform stretch (either uniaxial or equibiaxial) of smooth muscle cells (SMCs) and fibroblasts on elastic substrates (e.g., Refs. [2] and [3], respectively).

Such research has led to a greatly improved understanding of the types of mechanical cues cells are able to sense, how they are able to react, and the signaling molecules and mechanisms involved in transforming the mechanical input into a biological response (i.e., mechanotransduction). These responses include alignment, proliferation, apoptosis, protein expression, migration, and phenotype modulation (both differentiation and de-differentiation) [4,5]. Many of these behaviors are significant as they play key roles during disease progression. For instance during atherosclerosis development, smooth muscle cells migrate from the media to the intima wherein they settle, undergo a phenotype shift, and proliferate (intimal hyperplasia) [6]. This process can also occur after interventions with angioplasty or stenting (termed restenosis in these cases), resulting in treatment failure [7]. Fibroblast migration and differentiation has been implicated in arterial disease as well, as the adventitial cells contributed to neointima formation within injured porcine arteries [8]. More generally, fibroblast migration is crucial to wound repair in many tissue types within the body [9].

Despite the progress of past mechanobiological studies, a particular mechanical signal that has remained largely unaddressed is a gradient in stretch, rather than simply stretch magnitude. Applying internal pressure to a thick-walled incompressible tube results in a greater degree of stretching at the internal surface than the external. The resulting transmural gradient in stretch could potentially stimulate a cell response differently than just high or low stretch magnitudes. It is true that arteries are known to possess residual stresses, which act to homogenize the distribution of circumferential stress in idealized, straight artery models [10]. Still, this mechanism does not fully equalize stress distributions in all arteries. In the lateral wall of the carotid sinus, for example, inner wall stress is predicted to be four times that of the outer wall, even in the presence of residual stresses [11]. Intriguingly, the ratio of inner to outer wall stress correlated positively with early intimal thickening in this region [12].

Stress gradients in the artery wall can be exacerbated by several pathologic conditions as well. In hypertensive arteries, higher pressures generate greater stretching of the intima

Contributed by the Bioengineering Division of ASME for publication in the JOURNAL OF BIOMECHANICAL ENGINEERING. Manuscript received June 15, 2011; final manuscript received October 2, 2011; published online November 1, 2011. Assoc. Editor: Clark T. Hung.

compared to the adventitia [13]. Also, interventions aimed at restoring flow to blocked vessels (e.g., balloon angioplasty and stenting) are predicted by numerous groups to magnify transmural gradients in stress [14–17]. Thus, despite compensatory mechanisms such as residual stress, artery stresses are not always uniform across the wall, and a higher degree of non-uniformity (i.e., steeper gradient) is linked to conditions with altered cell behavior. We suppose that these gradients might be detected by arterial cells, which respond in ways that contribute to disease progression and treatment failure. It should be noted that other tissues can exhibit non-uniform stress and stretch-fields as well, for example, skin after the introduction of a defect or a rigid fixation such as a suture [18,19].

The notion that spatial distribution of mechanical signals can affect cell behavior has long been suggested, at least as early as Leung et al. [2] who, in concluding their landmark paper, identified "frequency, amplitude, or pattern of stress" as potential mechanical inputs for cell behavior. Supporting this hypothesis is the now well-known behavior of durotaxis, in which cells sense a gradient in stiffness of the substrate to which they are adhered and preferentially migrate toward stiffer regions [20]. If cells possess the molecular machinery necessary to detect a gradient in substrate stiffness, then it would seem that the same or similar machinery might potentially be equipped to detect a gradient not in stiffness but in stress or stretch. This idea is further supported by the work of Raeber et al. [21], who noted fibroblast migration rates to be greatest in regions of the steepest strain gradient. Balestrini et al. have presented the most detailed study of cells subjected to non-uniform stretching to date, but focused on the effects of "strain anisotropy" instead of gradients [22]. Despite suggestions that non-uniformity might play a role in mechanobiology, no study, to our knowledge, has decisively shown whether stretch gradients can act as a sufficient cue to modulate cell behavior.

We have designed and tested a device capable of stretching cells on elastomeric membranes with tunable spatial gradients in circumferential and radial stretch components. The device subjects cells to a non-uniform, biaxial stretch field by radially deforming a circular membrane with either a central defect or fixation boundary condition. Analyzing cell responses from various regions within the non-uniform fields will elucidate the effects of stretch gradients on disease-related cell behavior—a necessary task for a complete understanding of disease pathogenesis and important to the development of adequate treatment methods for cardiovascular disease, the leading cause of mortality in the United States [23]. Herein, we describe the device design and capabilities and present initial results of cell behavior as a feasibility test for future in vitro investigation.

Methods

Device Design and Construction. The cell-stretching device (shown in Fig. 1 and Fig. 2) uses a platen-displacement technique, as employed by others [3,24], to radially deform circular, elastomeric membranes. A membrane with a diameter of 80 mm is cut from 0.25 mm NRVG/G40D silicone sheeting, (Specialty Manufacturing Inc., Saginaw, WI) and clamped at its circumference to a Delrin ring. The ring suspends the membrane over a stationary, Teflon disc with rounded edges to facilitate smooth indentation. A stepper motor (Anaheim Automation, Anaheim, CA) is used to vertically displace the ring via a central post connector, which stretches the membrane over the disk with uniform radial deformation. The stepper motor is controlled by SMC50WIN software (Anaheim Automation) that allows programming of precise levels of static or cyclic stretching. Excluding the motor, the stretching mechanism is enclosed in a Lexan box and incubated to maintain cell culture medium at 37 °C and 5% CO_2. All device components can be sterilized by autoclave or UV exposure, and the assembled device fits on top of an inverted microscope for viewing through a cover slip mounted in the bottom of the culture box. By suspending the membrane over a stationary disc, cells can be kept in a constant focal plane for observation at any stretch level.

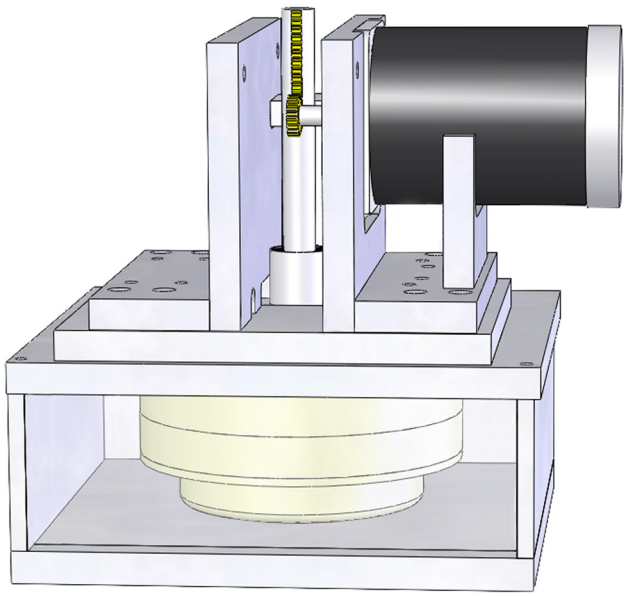

Fig. 1 Schematic of stretching device. A computer-controlled stepper motor drives radial deformation of a circular membrane via stretching over an indenter disk. The assembly can be mounted on an inverted microscope for imaging through a cover slip in the bottom of the box.

In order to generate gradients in stretch, either a circular defect (hole) or fixation will be placed at the center of the membrane. This method of producing non-uniform stretch environments is based upon previous computational work done by our lab as well as Humphrey and colleagues [18,19]. When circular elastomeric membranes are radially deformed, circumferential and radial stretches are generated. The addition of either a defect or a fixation at the center of the membrane generates gradients in these stretch components along the radial direction. The magnitude and shape of the stretch profile depend upon the size and type of the central boundary condition as well as the stretch imposed at the

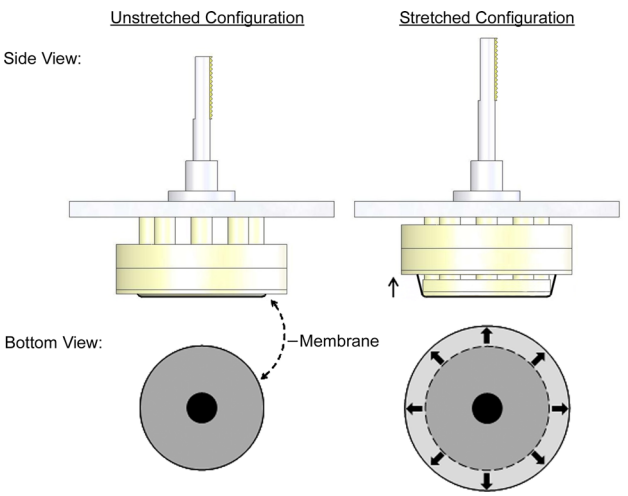

Fig. 2 Membrane deformation schematic. As the clamp ring is vertically displaced, the membrane is stretched over the stationary indenter disk. This action radially deforms the cell-seeded membrane while holding it at a constant focal plane for imaging.

Table 1 Gene descriptions and primer sequences for RT-PCR analysis of expression

Gene name	Abbr.	Function	Primer sequence
Biglycan	Bgn	Extracellular matrix component involved in deposition of collagens, cell adhesion, activation and inactivation of cytokines, and growth factors.	F: 5' – CGC CCT GGT CTT GGT AAA CA – 3' R: 5' – TTC CGC AGA GGG CTA AAC G – 3'
Caldesmon	Cald1	Calmodulin and actin-binding protein that plays an essential role in the regulation of smooth muscle and nonmuscle contraction.	F: 5' – AAC AAG TCA CCT GCT CCC AAG – 3' R: 5' – GAA GTG ACC TAT CCA CAG ATT GC – 3'
Calponin	CNN	Calcium binding protein that inhibits the ATPase activity of myosin in smooth muscle.	F: 5' – CGA TCC CAA GTA CTG CCT GAA – 3' R: 5' – TTG TGC GGG TGG TGA TTG – 3'
Early growth response 1	EGR1	DNA binding domain that functions as a transcriptional regulator.	F: 5' – GCC GAG ATG CAA TTG ATG TCT – 3' R: 5' – TGT CCA TGG TGG GTG AGT GA – 3'
FBJ osteosarcoma oncogene	cfos	An immediate early gene encoding a nuclear protein involved in signal transduction.	F: 5' – GGG AGG CCT TAC CTG TTC GT – 3' R: 5' – CAG ATG TGG ATG CTT GCA AGT C – 3'
Inhibitor of DNA binding 1	id1	Inhibits the DNA binding and transcriptional activation ability of basic HLH proteins with which it interacts. This protein may play a role in cell growth, senescence, and differentiation.	F: 5' – TGC TAC TCA CGC CTC AAG GA – 3' R: 5' – GGA TCT CCA CCT TGC TCA CTT T – 3'
Inhibitor of DNA binding 2	id2		F: 5' – CGC TGA CCA CCC TGA ACA C – 3' R: 5' – TCG ACA TAA GCT CAG AAG GGA AT – 3'
Integrin, alpha V	ITGAV	Joins with beta 3 to form a fibronectin receptor to participate in cell-surface mediated signaling.	F: 5' – CGA CAT TGA CGG GCC AAT – 3' R: 5' – CGC CGC TGT GTC ATT CTT TT – 3'
Integrin, beta 3	ITGB3	Beta unit of a fibronectin receptor to participate in cell-surface mediated signaling.	F: 5' – CGC ATC CCA TTT GCT AGT GTT – 3' R: 5' – GTC GGT GCC AAT GTG ACA GT – 3'
Plasminogen Activator Inhibitor-1	pai1	Inhibitor of fibrinolysis.	F: 5' – GGC ACA GTG GCG TCT TCC T – 3' R: 5' – TGC CGA ACC ACA AAG AGA AAG – 3'
Platelet derived growth factor beta	PDGFB	Mitogenic factor for cells of mesenchymal origin.	F: 5' – AGC TCG GGT GAC CAT TCG – 3' R: 5' – TCA TGG GTG TGC TTA AAC TTT CG – 3'
pro-Collagen 1	Procol1	Fibril-forming collagen found in most connective tissues abundant in bone, cornea, dermis, and tendon.	F: 5' – CCC CGG GAC TCC TGG ACT T – 3' R: 5' – GCT CCG ACA CGC CCT CTC TC – 3'
pro-Collagen 3	Procol3	A fibrillar collagen found in extensible connective tissues such as skin, lung, intestine and vasculature.	F: 5' – CCT GGA GCC CCT GGA CTA ATA G – 3' R: 5' – GCC CAT TTG CAC CAG GTT CT – 3'
SKI-like oncogene	SnoN	Negative regulator of TGFβ signaling. Binds to nuclear Smad complexes, repressing transcriptional activities.	F: 5' – ATA CAC CAT CGG GAA TGG AA – 3' R: 5' – CAT GAT CTT CCC CTT GTC GT – 3'
SMAD family member 1	Smad 1	Signal transducer and transcriptional modulator that mediates BMP signaling.	F: 5' – CCT GTG GCT TCC GTC TCT TG – 3' R: 5' – AAT AGT TGG TCA CAG AGG TCA AGT – 3'
SMAD family member 5	Smad 5	Receptor regulated SMAD involved in BMP signaling.	F: 5' – CAC GCT TTT GGT ATC TAC TGA CTT – 3' R: 5' – ATT TCT CTT CCT CGT CAC CTT GT – 3'
Smooth muscle Actin alpha 2	Acta2	Found in muscle tissues and are a major constituent of the contractile apparatus.	F: 5' – ACG AAC GCT TCC GCT GC – 3' R: 5' – GAT GCC CGC TGA CTC CAT – 3'
Smooth muscle Actin gamma 2	Actg2	Component of the cytoskeleton that acts as a mediator of internal cell motility.	F: 5' – GCC CTG GAT TTC GAG AAT GA – 3' R: 5' – CCA TCA GGC AAC TCG TAG CTT – 3'
Smoothelin	Smtn	Structural protein that is found exclusively in contractile smooth muscle cells. It associates with stress fibers and constitutes part of the cytoskeleton.	F: 5' – CGA GAG CCG AAG CAA TGT GG – 3' R: 5' – CGC TCG GTT TTG GTA ACT GTG – 3'

Table 1 *Continued*

Gene name	Abbr.	Function	Primer sequence
Snail homolog 1	Snail	Zinc finger transcriptional repressor downregulating expression of ectodermal genes within the mesoderm.	F: 5' – CAC CCT CAT CTG GGA CTC TC – 3' R: 5' – CTT CAC ATC CGA GTG GGT TT – 3'
Transgelin	TAGLN	A transformation and shape-change sensitive actin cross-linking/gelling protein found in fibroblasts and smooth muscle.	F: 5' – GAG GGA TCG AAG CCA GTG AA – 3' R: 5' – TGA GCC ACC TGT TCC ATC TG – 3'
Tropomyosin 1	TPM1	A highly conserved, widely distributed actin-binding protein involved in the contractile system of muscle cells and the cytoskeleton of non-muscle cells.	F: 5' – TGC TGA CCG GAA GTA TGA AG – 3' R: 5' – TCA AGT TGT TCG TCA CCG TT – 3'

outer circumference (based on the degree of vertical displacement, in our case). Defects are added to membranes using metal punches, and fixations are added by securing rigid rubber washers to the membranes' centers using Loctite 4206 medical device adhesive (Henkel Loctite Corp., Rocky Hill, CT).

Stretch Characterization. Stretch profiles producible by the device were characterized by marking membranes at various radial points and imaging at a range of motor displacements. Four cases were analyzed with varying boundary conditions, 2.8 mm defect, 8.0 mm defect, 2.2 mm fixation, and 6.8 mm fixation. The images were analyzed with ImageJ software (NIH) and positions calculated based on coordinates of the microscope stage and pixel coordinates within the image. Circumferential and radial stretch ratios were calculated as r/R (current/original radial position) and $\Delta r/\Delta R$, respectively. The resulting stretch data were used to find mechanical properties of the silicone membranes. Material parameters were estimated by fitting the data with the Mooney-Rivlin strain energy constitutive model in Eq. (1),

$$W = c_1(I_1 - 3) + c_2(I_2 - 3) \tag{1}$$

where W is the strain energy, I_1 and I_2 are the first and second invariants of the Right-Cauchy Green deformation tensor, and c_1 and c_2 are material parameters. The fitting procedure varied these parameters while iteratively solving the finite deformation problem as done previously [18], until a least squared error was achieved. Error was defined as the sum of the differences between experimental and theoretical circumferential stretch values at all loadings for both the small and large defect cases.

Cell Culture and Imaging. In order to demonstrate device feasibility for cell mechanobiology investigation, preliminary studies with fibroblasts and smooth muscle precursor cells were performed. For cell culture, both NIH 3T3 mouse fibroblasts (ATCC CRL-1658) and mouse 10T1/2 cells (ATCC CCL-226) were grown and maintained in Dulbecco's modified Eagles medium with 10% fetal bovine serum and 1% antibiotic-antimycotic (Invitrogen, Carlsbad, CA; Atlas Biologicals, Fort Collins, CO). 10T1/2 cells are a mesenchymal SMC line, traditionally used for phenotype studies due to the experimental ease of controlling their differentiation into mature SMCs [25]. Cultures were maintained at 37 °C and 5% CO_2.

Membranes with the large defect boundary condition were coated for a period of 2 h with bovine fibronectin (Sigma-Aldrich, St. Louis) diluted in PBS (Invitrogen) to a concentration of 50 μg mL^{-1}. Cells were labeled with DiI lipid stain according to manufacturer's protocol (Invitrogen), seeded at a density of 10^4 cm^{-2}, and allowed to adhere for 24 h. Subsequent to cell attachment, membranes were cyclically stretched for 24 h at 1 Hz and a medium-level loading (4% circumferential stretch at outer edge achieved by 5.0 mm vertical displacement of the clamped ring). A Nikon TE-2000 Inverted Fluorescent Microscope equipped with a Nikon C-FL FITC HYQ filter set (Nikon Instruments, NY) was used to image the cells at 40x magnification. Images of cell behavior at 20–25 selected locations were taken before and after stretching. A motorized stage was used to return to the same membrane positions in order to repeatedly image identical cells over time.

Cell Response Analysis: Gene Expression. The eventual purpose of this research is to link particular mechanical stimuli to cell behaviors; thus, we need to demonstrate the ability to measure such behaviors during and after stretching with the device while maintaining cell viability. In addition to imaging cells, gene expression for a variety of phenotype-related proteins was quantified using quantitative reverse-transcription polymerase chain reaction (RT-PCR) with primers to a number of genes representing various aspects of smooth muscle phenotypes (Table 1). Subsequent to 24 h of stretching, membranes were cut into two concentric circles representing the inner and outer regions of the membrane. These regions were selected according to the predicted stretch profiles in order to allow comparison between high and low stretch values coupled with high and low stretch gradients. RNA from stretched cells in each region was collected separately by lysing and scraping using the RNEasy kit (Qiagen) with one column DNase digestion. Primers were designed using Primer Express software (ABI) using GeneBank annotated sequences. Real time RT-PCR was performed with 2X SYBR® Green Mastermix (ABI). Expression levels were calculated using a $\Delta\Delta$Ct method with results normalized to GAPDH levels. The expression of a set of genes representing the differentiated phenotype (e.g., alpha smooth muscle actin, gamma smooth muscle actin, caldesmon, smoothelin), and the synthetic/proliferative phenotype (e.g. pro-collagen I, pro-collagen III, biglycan, c-Fos, Egr-1, PDGF β, SKI-like oncogene) were quantified for each region.

Gene expression experiments were repeated for a total of five runs; in addition to five control runs (i.e., cells cultured without stretch). For statistical analysis, a two-tailed, paired student's t-test was conducted on $\Delta\Delta$CT values comparing stretched cell expression to unstretched cell expression. Statistical significance was defined as $p < 0.05$.

Results

Device Capability: Stretch Characterization. To analyze the stretch environments produced by the device, marked positions on membranes were tracked and measured before and after

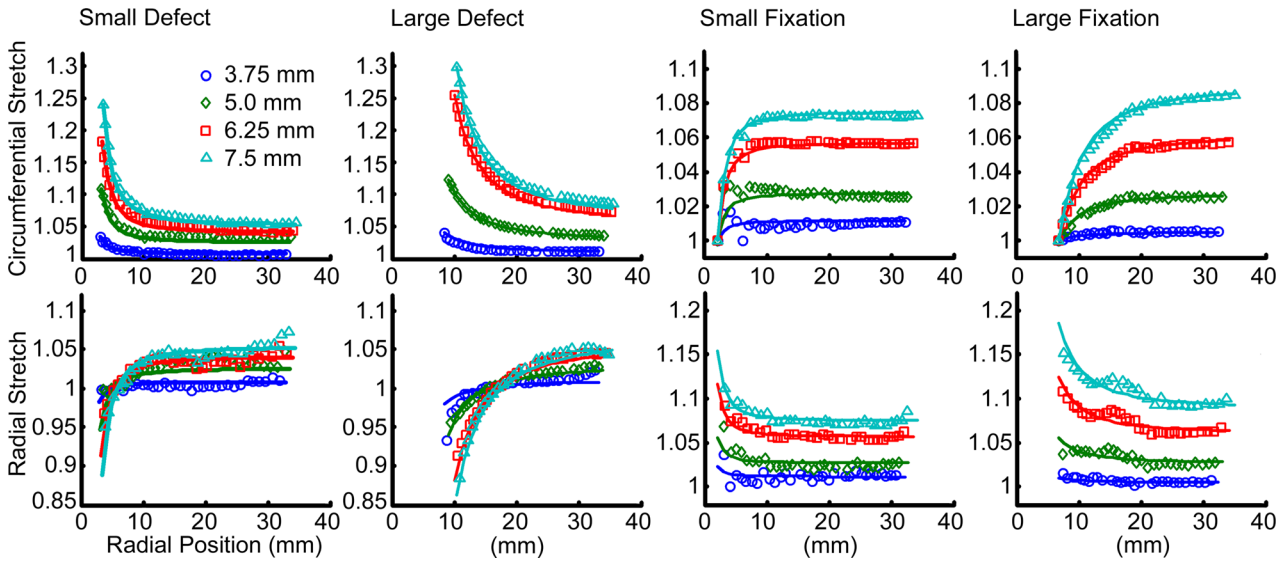

Fig. 3 Device stretching capabilities. Stretch profiles for defect and fixation (both small and large) central boundary conditions. Membranes were deformed by vertically displacing the clamped outer circumference at levels ranging from 3.75–7.5 mm. Stretch ratios were calculated from measured positions of marked points and fit by solving the corresponding finite deformation problem using a Mooney-Rivlin strain energy function.

deformation. The results match very closely to the curves predicted by the model solutions, and the membranes follow the expected behavior as predicted previously [18,19] (Fig. 3). For the defect cases, circumferential stretch ratio is greater than radial stretch ratio with the maximum difference occurring at the center edge. As radial position increases, circumferential stretch decreases (quickly at first, then more gradually) while radial stretch increases (in like manner) so that the outer edge is nearly equibiaxial. For the fixation cases, the same trend occurs but with the stretch components reversing places (i.e., radial stretch is greater and decreases with radial position, and circumferential stretch is lesser and increases with position).

The stretch profiles were modulated by varying the size of the inner boundary or the load placed on the membrane's outer circumference. Increasing the vertical displacement of the clamp ring from 3.75–7.5 mm expanded the ranges of stretch magnitude experienced across the membrane for all cases (Fig. 3). For a small defect at 3.75 mm displacement, circumferential stretch varied from 3.4% at the inner boundary to 0.7% at the outer. At 7.5 mm displacement, this range increased with circumferential stretch varying from 24.1% (inner) to 5.6% (outer). For a large defect, the same trends occur over greater ranges. For instance, circumferential stretch at 7.5 mm displacement varies from 29.8% at the inner boundary to 8.6% at the outer. Importantly, this variation across the membrane for a large defect occurs more gradually than for a small defect, resulting in profiles with less-steep gradients. At the inner boundary, circumferential stretch decreases 9.9% mm^{-1} with the small defect but only 6.1% mm^{-1} with the larger defect (both stretched with 7.5 mm displacement). The effects of loading and boundary size on stretch ranges and gradients are generally the same for fixation cases as well, though circumferential and radial stretch components are reversed in magnitude.

With the above characterization, experimental cases can be selected in order to isolate effects of point-wise stretch magnitude versus stretch gradient. For example, Fig. 4 shows the computed stretch profiles for defects and fixations of different radii (Ri = 2.8 or 8.0 mm for defect, and Ri = 2.2 or 6.8 mm for fixation). Regions have been identified (highlighted rectangles) that cover an identical range of circumferential and radial stretch magnitudes as well as the ratio between them but with drastically different gradients across that range (5.3% mm^{-1} for small defect versus 1.8% mm^{-1} for large defect, and 3.6% mm^{-1} for small fixation versus 1.1% mm^{-1} for large fixation). Thus, by comparing the cellular responses within each of these regions, the effects of stretch gradient can be revealed.

Cell Responses. To assess the feasibility of using the above stretches for cellular investigations, membranes with a large defect were seeded with either 3T3 fibroblasts or 10T1/2 cells and

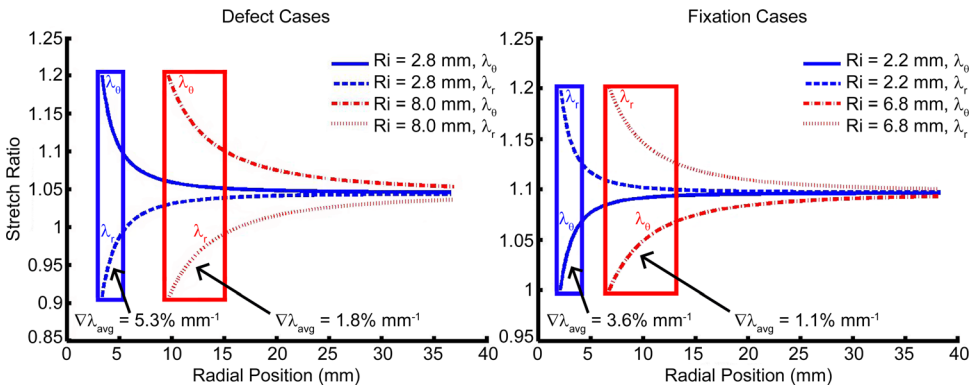

Fig. 4 Potential experimental stretching cases. Boxes highlight regions that span identical stretch magnitude ranges and anisotropy ratios, but different stretch gradients.

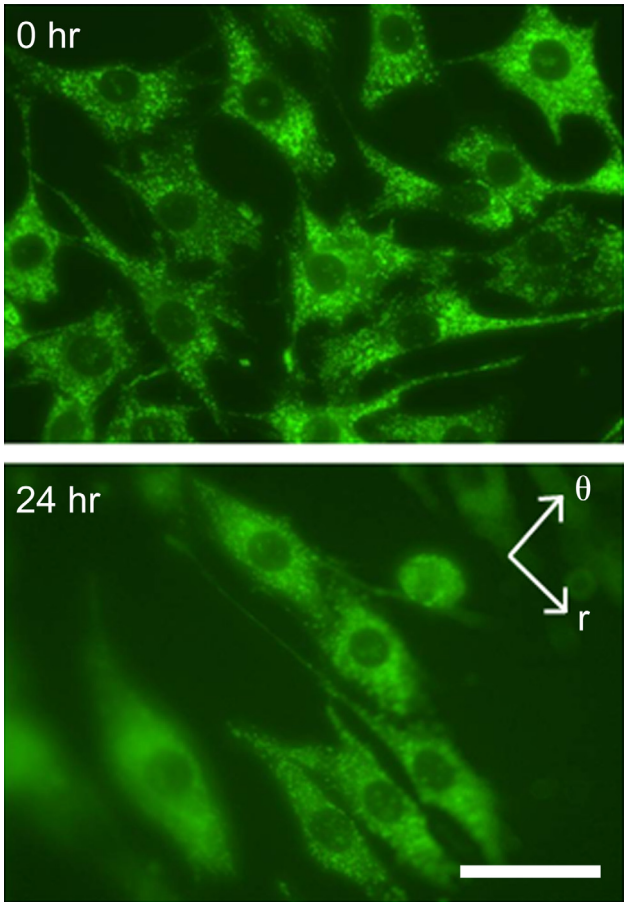

Fig. 5 3T3 fibroblast alignment in response to 24 h of cyclic stretch. Cells oriented perpendicular to their largest stretch component (circumferential stretch). Note that these images are not of identical cells but representative of the overall population. Scale bar is 50 μm.

cyclically stretched for 24 h from 0–4% outer circumferential stretch (5.0 mm vertical displacement) at a frequency of 1 Hz. Fluorescent images of both cell types after the stretching period showed healthy, viable cells still firmly attached to the substrate. Using memorized stage positions, we were able to locate the same groups of cells for imaging before and after stretching. There was a strong alignment tendency of fibroblasts in the radial direction as seen in Fig. 5, corresponding to the direction of lowest stretch.

Gene expression of phenotype-related proteins quantified by RT-PCR revealed a mix of contractile and synthetic markers affected to various degrees (Table 2). Over repeated experiments ($n = 5$), several mRNAs for genes associated with a mature contractile phenotype were downregulated including alpha-2-actin, gamma-2-actin, caldesmon, and alpha-V-integrin. However, other contractile phenotype markers were upregulated or unchanged (e.g., calponin, smoothelin, beta-3-integrin, and tropomyosin). Proteins associated with the de-differentiated, synthetic phenotype also showed mixed responses. Collagen III and collagen I were significantly downregulated, while SKI-like oncogene, EGR-1, and c-Fos were upregulated, and PDGF-beta remained unaffected by stretch. In most cases (except EGR-1 and c-Fos), there is little difference between expression in the inner and outer regions of the membrane. Recalling Fig. 3, these regions experience high circumferential stretch/high gradient, and lower circumferential stretch/low gradient, respectively.

Discussion

The primary aim of this research is to add tunable, physiologic gradients to a biaxial cell stretching environment, thereby providing a better reproduction of in vivo conditions. By deforming a circular elastomeric membrane modified with either a defect or fixation central boundary condition, we are able to generate a variety of stretch gradients to which cells can be subjected. Further, we present a novel method of experimental case selection to separate the effects of stretch magnitude from the effects of stretch gradient. Few other studies have aimed to study cell behavior in non-uniform stretch environments, and no other studies, to our knowledge, have clearly isolated the effects of a physiologic gradient on a particular response.

In the history of stretching experiments, a variety of devices have been used to subject SMCs to solid mechanical stress. The first and simplest of these devices deformed rectangular elastic substrates (seeded with cells) by clamping on opposite ends and uniaxially stretching [2]. Additional complexity and in vivo relevance has been achieved with biaxial stretching devices such as the Flexercell apparatus, which became commercially available in the 1990s (Flexcell Int., Cary NC). This design uses vacuum pressure to pull on the bottom of circular substrates in culture dishes, resulting in a biaxial (radial and circumferential) stretch environment. The stretch values generated with the Flexercell have been shown to vary tremendously depending on radial position [26]. However, the variation is a result of the device geometry and not a design feature. Thus, the gradients produced are not highly controllable and not physiologically relevant. The majority of researchers using those and other devices seek to homogenize the stretch field as much as possible in an attempt to better relate cell response to mechanical signals [3,24,27].

Recently, a few studies have developed novel devices for studying gradient effects. Ohashi et al. [28] subjected ECs to a gradient in strain magnitude by uniaxially deforming a rectangular membrane with a circular cover glass embedded into its center. They claim that stress fibers developed and nuclei localized at regions within a cell that were subjected to higher strain, supporting the hypothesis that cells can potentially sense and respond to subcellular variations in stretch. However, they do not quantify these behaviors, nor state whether this was the case for the majority of cells or just a sporadic finding. Yung et al. used a similar setup for their "cellular strain assessment tool," but after characterizing the mechanical environment of the uniaxial stretching device and quantifying an achievable gradient, the focus was returned to homogeneous strain environments with no mention of a plan for studying the effects of the gradient [29].

The most complete investigation of cell behavior in non-uniform stretching environments was conducted by Billiar and colleagues [22]. They also took the rigid inclusion approach, but did so in conjunction with the Flexercell device. Fixing a circular glass cover slip to the center of the circular substrate created gradients in radial and circumferential stretches across the radial position. Human dermal fibroblasts subjected to this environment for two days showed alignment perpendicular to maximal stretch. The extent of orientation varied with the cell's location on the substrate, presumably due to the local degree of "strain anisotropy," which they defined as $(\lambda_r - 1)/(\lambda_\theta - 1)$. This study effectively demonstrated the benefit of non-uniform environments in correlating cellular behavior to particular levels of stretch magnitude. In other words, a single experiment conducted on a non-uniform stretch field will illuminate cell responses at many various stretch levels. This can aid the generation of dose-response curves and improved mechanobiological models (a need that has been highlighted by recent reviews [30,31]), as well as help identify potential signaling thresholds. Still, Balestrini et al. [22] did not aim to reveal the effects of stretch non-uniformity on cell behavior, as they focused upon the effects of strain anisotropy. There remains a need to definitively test the ability of stretch gradients to elicit cellular responses.

The device presented herein, though similar to that presented by Balestrini et al. [22], improves upon previous cell-stretching systems by generating a large variety of non-uniform stretching profiles. Radially deforming a circular membrane with a central

Table 2 Gene expression of 10T1/2 cells quantified by RT-PCR. Cells were stretched for 24 h on a membrane with a large central defect. The membrane was separated into inner and outer concentric regions, and RNA was isolated from each region separately. Within the inner region, circumferential stretch (λ_θ) is high (1.1–1.15), radial stretch is low (<1), and stretch gradient (λ) is high. Within the outer region, circumferential stretch is lower (1.05–1.1) but still higher than radial stretch (1–1.05), and non-uniformity is lower. Only circumferential stretch and gradient qualities are reported in the table for simplicity. Genes are listed by the extent to which they were upregulated, downregulated, or insignificantly changed (relative to GAPDH expression) in response to stretch, when compared to a no-stretch control.

Gene	Region	Stretch-to-static expression ratio	Confidence interval	P value
Downregulated:				
Inhibitor of DNA binding 2	High λ_θ & High $\nabla\lambda$	0.11	(0.08, 0.15)	0.002
	Low λ_θ & Low $\nabla\lambda$	0.11	(0.09, 0.12)	0.001
Collagen III-α1	High λ_θ & High $\nabla\lambda$	0.20	(0.13, 0.32)	0.040
	Low λ_θ & Low $\nabla\lambda$	0.20	(0.13, 0.31)	0.064
Actin-α2	High λ_θ & High $\nabla\lambda$	0.23	(0.20, 0.26)	0.001
	Low λ_θ & Low $\nabla\lambda$	0.21	(0.18, 0.25)	0.001
Actin-γ2	High λ_θ & High $\nabla\lambda$	0.28	(0.15, 0.50)	0.160
	Low λ_θ & Low $\nabla\lambda$	0.37	(0.33, 0.42)	0.003
Collagen I-α2	High λ_θ & High $\nabla\lambda$	0.31	(0.24, 0.39)	0.015
	Low λ_θ & Low $\nabla\lambda$	0.40	(0.28, 0.58)	0.085
Caldesmon 1	High λ_θ & High $\nabla\lambda$	0.43	(0.39, 0.46)	0.002
	Low λ_θ & Low $\nabla\lambda$	0.45	(0.40, 0.50)	0.006
Inhibitor of DNA binding 1	High λ_θ & High $\nabla\lambda$	0.45	(0.36, 0.55)	0.016
	Low λ_θ & Low $\nabla\lambda$	0.44	(0.36, 0.54)	0.014
Integrin-αV	High λ_θ & High $\nabla\lambda$	0.61	(0.50, 0.74)	0.063
	Low λ_θ & Low $\nabla\lambda$	0.73	(0.66, 0.82)	0.043
Upregulated:				
Calponin 1	High λ_θ & High $\nabla\lambda$	17.06	(8.50, 34.22)	0.015
	Low λ_θ & Low $\nabla\lambda$	19.66	(11.50, 33.61)	0.005
Early growth response factor 1	High λ_θ & High $\nabla\lambda$	7.14	(3.77, 13.52)	0.037
	Low λ_θ & Low $\nabla\lambda$	4.33	(2.53, 7.41)	0.053
Serpin peptidase inhibitor 1	High λ_θ & High $\nabla\lambda$	3.70	(2.79, 4.90)	0.010
	Low λ_θ & Low $\nabla\lambda$	2.79	(1.94, 4.02)	0.048
c-Fos	High λ_θ & High $\nabla\lambda$	3.16	(2.65, 3.78)	0.008
	Low λ_θ & Low $\nabla\lambda$	1.78	(1.30, 2.43)	0.165
SKI-like oncogene	High λ_θ & High $\nabla\lambda$	2.08	(1.73, 2.49)	0.028
	Low λ_θ & Low $\nabla\lambda$	1.89	(1.73, 2.06)	0.002
Not significant ($p > 0.05$):				
Biglycan, Integrin-β3, MMP-2, PDGF-β, Smad1, Smad5, Smoothelin, Snail homolog 1, Transgelin, Tropomyosin 1				

fixation generates gradients in radial and circumferential stretch components. Our device can also employ a central defect boundary condition, which reverses the stretch components' relative magnitudes. It is noteworthy that the defect case better simulates the in vivo environment as it generates circumferential stretch greater than radial stretch, as well as a region of compressive radial stretch near the center. Both of these conditions are true in the native artery. Importantly, the magnitudes and gradients achievable by our device cover much of the range predicted in healthy arteries [11,32] during high-pressure angioplasty [14] and in atherosclerotic vessels [33], as listed in Table 3. By modulating the size of the central boundary, as well as the load placed on the membrane, stretch profiles spanning a variety of ranges with a variety of gradients can be produced. Careful selection between such cases allows the design of an experimental set of stretched membranes containing regions that span identical stretch magnitude ranges but with differing gradients. Though not illustrated, one could also select regions with identical gradients but covering different ranges of stretch magnitude. Moreover, we can compare defect cases to fixation cases of similar stretch and gradient in order to elucidate the differing effects (if any) created by radial stretch being the greater component versus circumferential stretch being the greater component.

The usefulness of a stretching device is ultimately dependent on its ability to elicit cell responses to various loading conditions. 3T3 fibroblasts stretched for 24 h showed strong alignment tendency in response to stretch. Cells on a membrane with a central defect aligned radially, which corresponded to the direction of lowest stretch. This finding agrees with the vast amount of literature that has shown both fibroblasts and SMCs orient perpendicular to the direction of maximal stress or strain [34–37]. The device is capable of employment in more detailed investigation of alignment behavior as well. In particular, it is possible that alignment is elevated in the presence of non-uniform stretch due to gradients acting as an additional directional cue. This will be an aim of future study.

To demonstrate the feasibility of the device in studying effects of stretch on SMC phenotype, 10T1/2 cells were stretched for 24 h and RT-PCR was used with a microarray to quantify gene expression. Fully differentiated vascular SMCs are characterized by a quiescent, strongly contractile state. However, they maintain a plasticity that allows them to respond to local environmental stimuli and undergo profound changes in phenotype. This characteristic plays an important role during development when SMCs help synthesize and assemble the extracellular matrix. The adult SMC are also able to respond to injury by phenotype modulation characterized by increased proliferation and synthesis and decreased expression of contractile proteins. The change in SMC phenotype from a differentiated contractile state to an undifferentiated synthetic state is a key process in the development and failed treatment of atherosclerosis, the deadliest disease in the US [23]. Unfortunately, it is evident from the disparity of previous studies that the effect of stretch on SMC phenotype is still very unclear.

Due to differences in the stretching environment, cell type, stretch amplitude, stretch frequency, and stretching duration, a number of groups over the past four decades have shown a "mixed bag" of results linking stretch to SMC phenotype [2,38–41]. These studies demonstrated varied cell behaviors with some stretching regimens causing a shift toward the synthetic state, some causing a shift toward the contractile state, and many causing cells to enter a hybrid phenotype where both synthetic and contractile proteins

Table 3 Computational estimates of stretch gradients under various conditions in vivo

Reference	Condition	Residual stress	Estimated $\mathbf{V}\lambda_{max}$
Delfino et al. [12]	Carotid bifurcation	Yes	13.4 (%/mm)
Younis et al. [32]	Carotid bifurcation	No	12.4
		Yes	5.0
Holzapfel & Gasser [14]	Balloon angioplasty during…		
	Inflation	Yes	2.3
	Peak Pressure	Yes	13.2
	Deflation	Yes	8.1
Hayashi & Imai [33]	Atherosclerotic artery at…		
	160 mmHg	No	81.5
	120 mmHg	No	53.6
Proposed Device	—	—	*≤22.0*

are produced. It seems that 10T1/2 cells in our system indeed express a sort of hybrid phenotype, up and down-regulating proteins related to both states of differentiation. In most cases, these changes in expression were significant over unstretched control cells. However, with the exceptions of EGR-1 and c-Fos, there was not much difference between cell expression in the inner and outer regions corresponding to high circumferential stretch/high gradient and lower circumferential stretch/low gradient, respectively. This could be directly due to a lack of cell-sensitivity to the difference in mechanical signals between those regions, or indirectly due to paracrine effects in the media. In either case, future studies can use more varied mechanical stimuli and employ controls that are treated with the same media in order to reveal more precisely the effects of stretch and stretch gradient on SMC gene expression and phenotype shift.

Cell alignment and gene expression for phenotype-related proteins were evaluated, herein, as straight-forward preliminary studies demonstrating the feasibility of experimentation with the device design. Future studies will add considerable detail to alignment and expression responses including the effect, if any, of stretch gradients. Additionally, the device is capable for investigation of many other cell behaviors. SMC migration, in particular, is of interest as a contributor to intimal hyperplasia in atherogenesis and restenosis. SMCs often migrate from the media to the intima in such conditions, contributing to the neointima, which can eventually lead to vessel occlusion [6,42]. As mentioned previously, SMCs have been shown to migrate in response to gradients of substrate stiffness, suggesting the possibility that this behavior could also occur in response to gradients in stretch. Our device is perfectly suited to investigate such behavior, as cells can be subjected to various degrees of gradient while tracking individual cell positions over time for imaging and migration quantification.

A primary limitation of this work is the use of 2D cell culture as a simulation of true in vivo behavior. Cells within the body are under complex 3D stimuli of many kinds, all important and working in balance to achieve a response. Though the 2D environment is simplified, we still feel that it holds much investigative power as it allows us to precisely control some of these stimuli and isolate particular behaviors related to them. Moreover, our device can be adapted to stretching 3D constructs. In preliminary work not shown, PEG-DA hydrogels have been mounted on this device and stretched to levels of 10% without construct failure. Therefore, we aim to extend investigations into 3D geometries as we incrementally approach the in vivo environment.

In summary, we have designed and tested a cell-stretching device for novel investigation of the effects of stretch gradients on cell behavior. By radially deforming an elastomeric, circular membrane with either a central defect or rigid fixation, gradients in biaxial stretch components are generated. These gradients can be fine-tuned by varying the type and size of the boundary condition as well as the load placed on the outer circumference of the membrane. Thus, experimental cases were identified that can separate the effects of stretch magnitude from the effects of stretch gradient. Both 3T3 fibroblasts and 10T1/2 cells were subjected to a sample stretching regimen and displayed good viability while altering their orientation and phenotype-related protein expression. Future studies will use a thorough combination of stretch conditions to identify the effect of non-uniform stretches on cell alignment, phenotype modulation, and migration. Such work would be the first to prove stretch gradients as sufficient cues to affect cell behavior, linking this mechanical signal to in vivo cellular adaptations leading to disease progression. Understanding these pathological processes would enable a more accurately targeted treatment to heal or inhibit disease, either through implantable device design or pharmaceutical delivery.

Acknowledgment

The authors gratefully acknowledge Dr. Daisuke Mori for help during device conception, Mr. David Howell for help with cell culture and Table 1 (RT-PCR gene descriptions), Mrs. Shiva Yazdani-Beioky for preliminary testing of the device, and the Carolyn S. and Tommie E. Lohman '59 Professorship for the support of JEM.

Nomenclature

EC = endothelial cell
I_1 = first invariant of the Right-Cauchy Green deformation tensor
I_2 = second invariants of the Right-Cauchy Green deformation tensor
PBS = phosphate-buffered saline
Ri = original inner radius of membrane boundary
$RT\text{-}PCR$ = reverse transcription polymerase chain reaction
SMC = smooth muscle cell
W = mechanical strain energy function
c_1 = material parameter in strain energy function
c_2 = material parameter in strain energy function
r/R = current/original radial position
λ_θ = circumferential stretch
λ_r = radial stretch
$\mathbf{V}\lambda$ = stretch gradient

References

[1] Levesque, M. J., and Nerem, R. M., 1985, "The Elongation and Orientation of Cultured Endothelial Cells in Response to Shear Stress," J. Biomech. Eng., **107**(4), pp. 341–347.
[2] Leung, D. Y., Glagov, S., and Mathews, M. B., 1976, "Cyclic Stretching Stimulates Synthesis of Matrix Components by Arterial Smooth Muscle Cells in vitro," Science, **191**(4226), pp. 475–477.
[3] Lee, A. A., Delhaas, T., Waldman, L. K., MacKenna, D. A., Villarreal, F. J., and McCulloch, A. D., 1996, "An Equibiaxial Strain System for Cultured Cells," Am. J. Physiol., **271**(4), pp. C1400–1408.
[4] Wang, J. H., and Thampatty, B. P., 2006, "An Introductory Review of Cell Mechanobiology," Biomech. Model. Mechanobiol., **5**(1), pp. 1–16.
[5] Haga, J. H., Li, Y. S., and Chien, S., 2007, "Molecular Basis of the Effects of Mechanical Stretch on Vascular Smooth Muscle Cells," J. Biomech., **40**(5), pp. 947–960.
[6] Rudijanto, A., 2007, "The Role of Vascular Smooth Muscle Cells on the Pathogenesis of Atherosclerosis," Acta Med. Indones., **39**(2), pp. 86–93.

[7] Mitra, A. K., and Agrawal, D. K., 2006, "In Stent Restenosis: Bane of the Stent Era," J. Clin. Pathol., **59**(3), pp. 232–239.
[8] Shi, Y., O'Brien, J. E., Fard, A., Mannion, J. D., Wang, D., and Zalewski, A., 1996, "Adventitial Myofibroblasts Contribute to Neointimal Formation in Injured Porcine Coronary Arteries," Circulation, **94**(7), pp. 1655–1664.
[9] Mutsaers, S. E., Bishop, J. E., McGrouther, G., and Laurent, G. J., 1997, "Mechanisms of Tissue Repair: From Wound Healing to Fibrosis," Int. J. Biochem. Cell Biol., **29**(1), pp. 5–17.
[10] Chuong, C. J., and Fung, Y. C., 1986, "On Residual Stresses in Arteries," J. Biomech. Eng., **108**(2), pp. 189–192.
[11] Delfino, A., Stergiopulos, N., Moore, J. E., Jr., and Meister, J. J., 1997, "Residual Strain Effects on the Stress Field in a Thick Wall Finite Element Model of the Human Carotid Bifurcation," J. Biomech., **30**(8), pp. 777–786.
[12] Delfino, A., Moore, J. E., Stergiopulos, N., Vaclavik, V., Genton, C. Y., and Meister, J. J., 1998, "Wall Stresses in the Carotid Bifurcation: Effects of Wall Non-Homogeneity and Correlation With Intimal Thickness," J. Vasc. Invest., **4**(2), p. 11.
[13] Matsumoto, T., and Hayashi, K., 1996, "Stress and Strain Distribution in Hypertensive and Normotensive Rat Aorta Considering Residual Strain," J. Biomech. Eng., **118**(1), pp. 62–73.
[14] Holzapfel, G. A., and Gasser, T. C., 2007, "Computational Stress-Deformation Analysis of Arterial Walls Including High-Pressure Response," Int. J. Cardiol., **116**(1), pp. 78–85.
[15] Bedoya, J., Meyer, C. A., Timmins, L. H., Moreno, M. R., and Moore, J. E., 2006, "Effects of Stent Design Parameters on Normal Artery Wall Mechanics," J. Biomech. Eng., **128**(5), pp. 757–765.
[16] Kiousis, D. E., Gasser, T. C., and Holzapfel, G. A., 2007, "A Numerical Model to Study the Interaction of Vascular Stents With Human Atherosclerotic Lesions," Ann. Biomed. Eng., **35**(11), pp. 1857–1869.
[17] Lally, C., Dolan, F., and Prendergast, P. J., 2005, "Cardiovascular Stent Design and Vessel Stresses: A Finite Element Analysis," J. Biomech., **38**(8), pp. 1574–1581.
[18] David, G., and Humphrey, J. D., 2004, "Redistribution of Stress due to a Circular Hole in a Nonlinear Anisotropic Membrane," J. Biomech., **37**(8), pp. 1197–1203.
[19] Mori, D., David, G., Humphrey, J. D., and Moore, J. E., Jr., 2005, "Stress Distribution in a Circular Membrane With a Central Fixation," J. Biomech. Eng., **127**(3), pp. 549–553.
[20] Lo, C. M., Wang, H. B., Dembo, M., and Wang, Y. L., 2000, "Cell Movement is Guided by the Rigidity of the Substrate," Biophys. J., **79**(1), pp. 144–152.
[21] Raeber, G. P., Lutolf, M. P., and Hubbell, J. A., 2008, "Part II: Fibroblasts Preferentially Migrate in the Direction of Principal Strain," Biomech. Model. Mechanobiol., **7**(3), pp. 215–225.
[22] Balestrini, J. L., Skorinko, J. K., Hera, A., Gaudette, G. R., and Billiar, K. L., 2010, "Applying Controlled Non-Uniform Deformation for in Vitro Studies of Cell Mechanobiology," Biomech. Model. Mechanobiol., **9**(3), pp. 329–344.
[23] Lloyd-Jones, D., Adams, R. J., Brown, T. M., Carnethon, M., Dai, S., De Simone, G., Ferguson, T. B., Ford, E., Furie, K., Gillespie, C., Go, A., Greenlund, K., Haase, N., Hailpern, S., Ho, P. M., Howard, V., Kissela, B., Kittner, S., Lackland, D., Lisabeth, L., Marelli, A., McDermott, M. M., Meigs, J., Mozaffarian, D., Mussolino, M., Nichol, G., Roger, V. L., Rosamond, W., Sacco, R., Sorlie, P., Thom, T., Wasserthiel-Smoller, S., Wong, N. D., and Wylie-Rosett, J., 2010, "Heart Disease and Stroke Statistics–2010 Update: A Report From the American Heart Association," Circulation, **121**(7), pp. e46–e215.
[24] Huang, L., Mathieu, P. S., and Helmke, B. P., 2010, "A Stretching Device for High-Resolution Live-Cell Imaging," Ann. Biomed. Eng., **38**(5), pp. 1728–1740.
[25] Hirschi, K. K., Lai, L., Belaguli, N. S., Dean, D. A., Schwartz, R. J., and Zimmer, W. E., 2002, "Transforming Growth Factor-Beta Induction of Smooth Muscle Cell Phenotype Requires Transcriptional and Post-Transcriptional Control of Serum Response Factor," J. Biol. Chem., **277**(8), pp. 6287–6295.
[26] Vande Geest, J. P., Di Martino, E. S., and Vorp, D. A., 2004, "An Analysis of the Complete Strain Field Within Flexercell Membranes," J. Biomech., **37**(12), pp. 1923–1928.
[27] Brown, T. D., 2000, "Techniques for Mechanical Stimulation of Cells in Vitro: A Review," J. Biomech., **33**(1), pp. 3–14.
[28] Ohashi, T., Masuda, M., Matsumoto, T., and Sato, M., 2007, "Nonuniform Strain of Substrate Induces Local Development of Stress Fibers in Endothelial Cells Under Uniaxial Cyclic Stretching," Clin. Hemorheol. Microcirc., **37**(1–2), pp. 37–46.
[29] Yung, Y. C., Vandenburgh, H., and Mooney, D. J., 2009, "Cellular Strain Assessment Tool (CSAT): Precision-Controlled Cyclic Uniaxial Tensile Loading," J. Biomech., **42**(2), pp. 178–182.
[30] Moore, J. E., Jr., 2009, "Biomechanical Issues in Endovascular Device Design," J. Endovasc. Ther., **16**(1 Suppl), pp. I1–11.
[31] Humphrey, J. D., 2008, "Vascular Adaptation and Mechanical Homeostasis at Tissue, Cellular, and Sub-Cellular Levels," Cell Biochem. Biophys., **50**(2), pp. 53–78.
[32] Younis, H. F., Kaazempur-Mofrad, M. R., Chan, R. C., Isasi, A. G., Hinton, D. P., Chau, A. H., Kim, L. A., and Kamm, R. D., 2004, "Hemodynamics and Wall Mechanics in Human Carotid Bifurcation and its Consequences for Atherogenesis: Investigation of Inter-Individual Variation," Biomech. Model. Mechanobiol., **3**(1), pp. 17–32.
[33] Hayashi, K., and Imai, Y., 1997, "Tensile Property of Atheromatous Plaque and an Analysis of Stress in Atherosclerotic Wall," J. Biomech., **30**(6), pp. 573–579.
[34] Buck, R. C., 1980, "Reorientation Response of Cells to Repeated Stretch and Recoil of the Substratum," Exp. Cell Res., **127**(2), pp. 470–474.
[35] Dartsch, P. C., Hammerle, H., and Betz, E., 1986, "Orientation of Cultured Arterial Smooth Muscle Cells Growing on Cyclically Stretched Substrates," Acta Anat. (Basel), **125**(2), pp. 108–113.
[36] Kanda, K., Matsuda, T., and Oka, T., 1992, "Two-Dimensional Orientational Response of Smooth Muscle Cells to Cyclic Stretching," ASAIO J., **38**(3), pp. M382–385.
[37] Houtchens, G. R., Foster, M. D., Desai, T. A., Morgan, E. F., and Wong, J. Y., 2008, "Combined Effects of Microtopography and Cyclic Strain on Vascular Smooth Muscle Cell Orientation," J. Biomech., **41**(4), pp. 762–769.
[38] Morawietz, H., Ma, Y. H., Vives, F., Wilson, E., Sukhatme, V. P., Holtz, J., and Ives, H. E., 1999, "Rapid Induction and Translocation of Egr-1 in Response to Mechanical Strain in Vascular Smooth Muscle Cells," Circ. Res., **84**(6), pp. 678–687.
[39] Birukov, K. G., Shirinsky, V. P., Stepanova, O. V., Tkachuk, V. A., Hahn, A. W., Resink, T. J., and Smirnov, V. N., 1995, "Stretch Affects Phenotype and Proliferation of Vascular Smooth Muscle Cells," Mol. Cell. Biochem., **144**(2), pp. 131–139.
[40] Butcher, J. T., Barrett, B. C., and Nerem, R. M., 2006, "Equibiaxial Strain Stimulates Fibroblastic Phenotype Shift in Smooth Muscle Cells in an Engineered Tissue Model of the Aortic Wall," Biomaterials, **27**(30), pp. 5252–5258.
[41] Goldman, J., Zhong, L., and Liu, S. Q., 2003, "Degradation of Alpha-Actin Filaments in Venous Smooth Muscle Cells in Response to Mechanical Stretch," Am. J. Physiol. Heart Circ. Physiol., **284**(5), pp. H1839–1847.
[42] Schwartz, S. M., 1997, "Smooth Muscle Migration in Atherosclerosis and Restenosis," J. Clin. Invest., **100**(11 Suppl), pp. S87–89.